DFT cluster modeling of molecular and dissociative hydrogen adsorption on Zn^{2+} ions with distant placing of aluminum in the framework of high-silica zeolites

A.A. Shubin[a,*], G.M. Zhidomirov[a], V.B. Kazansky[b], and R.A. van Santen[c]

[a]*Boreskov Institute of Catalysis, Siberian Branch of the Russian Academy of Sciences, Pr. Akad. Lavrentieva 5, Novosibirsk 630090*
[b]*Zelinsky Institute of Organic Chemistry of Russian Academy of Sciences, Leninsky Prospect 47, Moscow 117913, Russia*
[c]*Schuit Institute of Catalysis, Eindhoven University of Technology, P.O. Box 513, 5600 MB, Eindhoven, The Netherlands*

Received 19 November 2002; accpted 10 July 2003

The problem of various cationic positions in zeolites with high Si/Al ratio in the framework is discussed. The statistical distribution of aluminum in the lattice of pentasils makes probable appearance of the structures with distant placing of two aluminum atoms. Cations, localized at such sites, should be very strong Lewis acids that are highly active in different chemical reactions. An example of such a site is considered for two Zn^{2+} ions stabilized in the zeolite fragment represented by two adjacent five-membered rings sharing the common edge. DFT calculations of molecular and dissociative hydrogen adsorption by such sites are in agreement with experimental results. Adsorption of dihydrogen by zinc ion at such sites results in an unusually large low-frequency shift of H–H stretching vibrations indicating essential activation of adsorbed H_2 molecule. The calculated path of heterolytic dissociative adsorption of dihydrogen and of the proton migration to the distantly placed basic oxygen of such acid-base pair are in agreement with the previously published DRIFT experimental data.

KEY WORDS: adsorption of dihydrogen; DFT calculations; Zn zeolite.

1. Introduction

It is generally believed that stabilization of bivalent metal cations in high-silica zeolites occurs at the sites containing two Al-occupied oxygen tetrahedra in the vicinity of each other. Therefore, the fraction of alumium ions in the next nearest positions (NNA sites) is an important characteristic of aluminum distribution in the framework of high-silica zeolites [1–3].

The dependence of the fraction of NNA sites from the average Si/Al ratio in the zeolite framework was discussed in reference [4]. Taking into account that according to the Löwenstein's rule the distances between two aluminum ions in the next nearest positions for ZSM-5 zeolite are in the range of 4.6–6 Å, it was concluded that for Si/Al > 50 the fraction of the NNA sites is less than 0.2. The more accurate calculation of the NNA distance using the ensemble averaging of aluminum distributions gave the close result [5]. Therefore, in zeolites with very high Si/Al ratios, the number of exchangeable bivalent cations at the sites with the pairing aluminum atoms in the framework should be either much less than the total aluminum content, or in addition to this model, stabilization of bivalent cations at the sites with the larger distance between adjacent aluminum ions should be also considered.

* To whom correspondence should be addressed.
E-mail: A.A.Shubin@catalysis.nsk.su

One of such possibilities is provided by formation of oxygen-bridged binuclear structures. For Zn^{2+} ions, this was discussed in reference [6], where the stabilization of $(Zn–O–Zn)^{2+}$ oxo-ions in the zeolite fragment represented by two adjacent five-membered rings sharing the common edge, with the distance between two aluminum ions being more than 7.5 Å was considered.

Another possibility is represented by the structures with alternation in the zeolite framework of positive and negative electric charges. In this case, the bivalent cations could be stabilized at the single negatively charged Al-occupied oxygen tetrahedra creating the sites with the excessive positive charge. Then, the equivalent amount of the lattice negative charges of the framework aluminum atoms with cationic vacancies should be compensated in the indirect way by electrostatic interaction with the surrounding local positive charges created by bivalent cations.

The experimental criterion of this model is the ability to replace all acidic protons in a high-silica zeolite by bivalent cations. Recently, we did this for the ZSM-5 zeolite with the Si/Al ratio of 25. All of the bridging hydroxyl groups were replaced in this case by the bivalent zinc ions via a high-temperature reaction with zinc vapor [7,8]. In agreement with the above discussion, this result should be considered as the first experimental evidence of the sitting of zinc cations in the zeolite framework at the single negative lattice charges created by the isolated aluminum atoms.

1011-372X/03/1000–0137/0

The important feature of such charge alternation models should be the very strong perturbation of adsorbed molecules by the bivalent cations with the excessive local positive charges. This is consistent with the results of our recent density functional theory (DFT) calculations, which indicated that the lower stability of Zn^{2+} ions at cationic sites in zeolites results in the easier dissociative adsorption of water and ethane [9]. In addition, the DFT calculations also demonstrated that dihydrogen and methane adsorption at the sites with separated charges should result in a very large perturbation of the adsorbed molecules [10]. It is important that the calculations did not predict such strong perturbation owing to the adsorption of these molecules on binuclear $(Zn–O–Zn)^{2+}$ oxo-ions [10–12].

Our previous experimental study of hydrogen adsorption on Zn- and Co-loaded ZSM-5 zeolites also indicated that diffuse reflectance infrared Fourier transform (DRIFT) spectra of these molecules are surprisingly different from those adsorbed by the faujusites modified with the same cations [7,8,13–15]. For instance, the H_2 adsorption by ZnHZSM-5 at 77 K results in the low-frequency shift of H–H stretching vibration equals to 220 cm^{-1}. This is almost twice as large as the low-frequency shift of H–H stretching frequency of 123 cm^{-1} for hydrogen adsorbed by Zn^{2+} ions at S_{II} sites in the six-membered rings of the ZnY zeolite [16]. In addition, zinc-loaded ZSM-5 dissociatively adsorbs molecular hydrogen at room temperature [7,8,13,15], indicating the low activation energy of heterolytic dissociation due to extremely high chemical activity of zinc ions. In accordance with the above discussion, it was also found that the most strongly low-frequency-shifted bands of adsorbed hydrogen are observed for the zeolites with the very high Si/Al ratios, where the distant placing of aluminum ions is most probable.

Zn-loaded ZSM-5 zeolite also unusually strongly perturbs adsorbed methane at room temperature. Upon adsorption, the band of symmetric C–H stretching vibrations becomes optically active and very intense with the low-frequency shift of about 100 cm^{-1}. This is also considerably larger than the low-frequency shift resulting from methane adsorption on Zn^{2+} ions at S_{II} sites in ZnY [14].

Similar results on the very strong perturbation of adsorbed molecular hydrogen were also obtained for low-temperature hydrogen adsorption on ZSM-5 zeolites modified with Co^{2+} ions [17]. Similar to the Zn-loaded zeolites, the strongest perturbation of adsorbed hydrogen was also observed for the samples with the highest Si/Al ratio of 40 or 80. In this case, the low-frequency shift of H–H stretching vibrations of 265 cm^{-1} was even larger than for hydrogen adsorption on ZnZSM-5.

In accordance with the above discussion and with the above-mentioned experimental results, we continue discussion of the nature of the sites with the distant placing of aluminum ions in high silica and of molecular and dissociative adsorption of hydrogen on these sites reported in references [7,8,13,15].

2. Computational details

Two adjacent five-membered rings on the wall of the straight channel of ZSM-5 zeolite have been suggested as a possible cationic site for the zinc ion with aluminum ions placed in T_{12} and T_8 lattice positions [18]. The distance between two aluminum ions at these positions is equal to 7.78 Å. The $ZnAl_2Si_6O_9H^*_{14}$ cluster shown in figure 1 was chosen for the model DFT calculations. Similar to [6], this structure will designated as Z_dZn in the following discussion. Hydrogen atoms (H^*) were used to saturate the dangling Si–O bonds at the border of the cluster. The starting geometry of the cluster corresponded to the real lattice of the ZSM-5 zeolite detected by XRD data.

DFT calculations were carried out using the GAUSSIAN-98 program [19] with B3LYP hybrid functional [20]. It accounts for the Hartree–Fock exchange, for a mixture of exchange and correlation functionals including gradient corrections of the electron density, and for the carefully chosen empirical parameters obtained from fitting of calculated values to accurate experimental data. Earlier, the hybrid B3LYP method has been reported to provide excellent descriptions of various reaction profiles, particularly of geometries, the heats of reactions, the barrier heights, and of vibrational analyses [21].

In the course of simulation of H_2 interaction with zinc ion at such cationic positions, the 6-31G* basis set was used for zinc and the 6-311G** basis set was used for H_2 for the zeolite oxygen atoms, and hydrogen atoms of bridging hydroxyl groups. Zeolitic Al and Si atoms, as well as H^* hydrogen atoms saturating the broken Si–O bonds at the edges of the cluster were treated with D95-Dunning/Huzinaga basis set. Such compromise choice allowed us to save computational time and, at the same time, to use the extended models

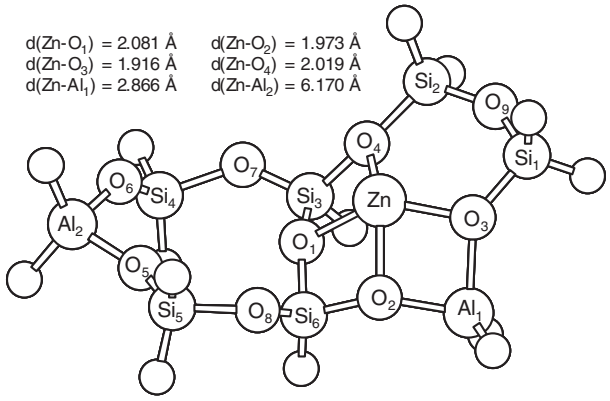

Figure 1. Optimized structure of two connected five-membered rings cluster $ZnAl_2Si_6O_9H^*_{14}(Z_dZn)$.

for frequency calculations without significant loss of accuracy.

Special restrictions were imposed on the optimization of positions of the boundary H* atoms. At the first step of the optimization procedure, the geometry of the entire zeolite cluster was chosen according to experimental X-ray diffraction data [18]. Only Si–H* and Al–H* bond distances were optimized, while the positions of other atoms (except Zn) as well as directions of O–H* bonds were fixed according to crystallographic data. The Zn^{2+} ion was allowed to move in this structure freely. Positions of H* atoms obtained after the first step of optimization procedure were saved and used further in the restricted geometry optimizations of H-forms and other zeolite structures with two connected 5-rings. The subsequent second step of optimization was performed with the fixed positions of H* atoms.

3. Results and discussion

The cluster discussed above is shown in figure 1. As could be expected, zinc cation is localized closer to one of aluminum ions with the longer distance to the other. Though the effective coordination number of Zn^{2+} by the zeolitic oxygen ions is four, the bond lengths with the two oxygen ions adjacent to aluminum are somewhat shorter than two others (figure 1). Evidently, the trapping of Zn^2 ion in the discussed cation position with the distant placing of aluminum ions (Z_d) is less stable than in the cases of cation position with closely placed Al^{3+} in the zeolite lattice (Z_s) or in the case of binuclear oxo-bridged structure $(Zn–O–Zn)^{2+}$ in the Z_d position [6]. This results in higher adsorption activity of Zn^2 ion according to previous common consideration [9]. The calculated lowest unoccupied molecular orbital (LUMO) energies for Z_dZn (−4.1 eV), Z_sZn (−3.2 eV), and Z_dZn_2O (−2.8 eV) clearly indicate that Lewis acidity strongly decreases in this order [6]. It explains the promoted ability of the discussed Z_dZn site in adsorption and activation of dihydrogen.

The calculated structure of molecular hydrogen adsorption by such a cluster is shown in figure 2. The obtained adsorption energy of H_2, 7.7 kcal/mol, is a reasonable value for H_2 interaction with the strong Lewis acid sites [12], and the electron charge transfer from H_2 on the adsorption site is 0.1*e*. Activation of H_2

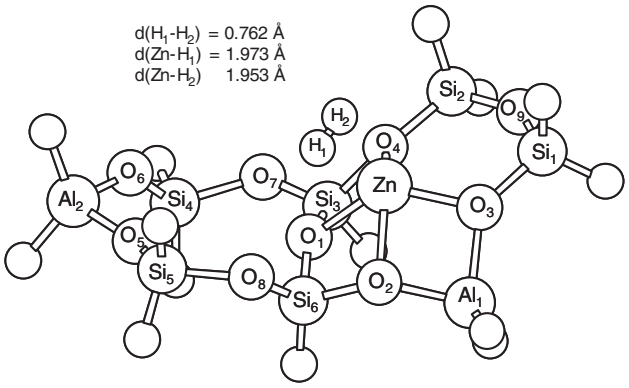

Figure 2. Molecular adsorption of H_2 on Z_dZn cluster.

is evident from the somewhat longer H–H bond in comparison with the calculated bond length for the free H_2 molecule (0.762 and 0.744 Å, respectively) and from the much lower H–H stretching frequency (See also table 1). The latter is lower by 270 cm^{-1} than that calculated under the same assumptions for free hydrogen molecule. These are the stimulating factors for the consequent heterolytic dissociative adsorption.

The first step of hydrogen dissociation involves the migration of proton to one of the adjacent oxygen ions of the zeolite framework, whereas the second hydrogen atom forms the hydride bond with the zinc ion. According to computational analysis, one of the possible targets for the migration of hydrogen atom is the framework basic $O_{(8)}$ oxygen ion (figure 2). The structure of the corresponding transition state with the H–H distance increased up to 1.025 Å is shown in figure 3. The atomic charges of hydrogen atoms in are equal to +0.322 ($H_{(1)}$) and −0.229 ($H_{(2)}$), in agreement with heterolytic path of dissociation. The resulting structure for the first step of H_2 dissociation is shown in figure 4. In this structure, the newly formed O–H bond is directed outward of the Z_dZn cluster.

This structure certainly is not final. The most stable sites of localization of the $H_{(1)}$ proton are the negatively charged basic oxygen ions connected with $Al_{(2)}$. Therefore, the next intermediate step of $H_{(1)}$ migration is "rotation" of $O_{(8)}$–$H_{(1)}$ bond around the quasilinear $Si_{(5)}$–$O_{(8)}$–$Si_{(6)}$ fragment in order to form the starting position for the subsequent step of proton migration (see energy diagram in figure 8 and also figure 5). The resulting structure for the second step of $H_{(1)}$ proton

Table 1
Calculated IR vibrational frequencies (cm^{-1}) for free H_2 and H_2 adsorbed (dissociated) on Z_dZn cluster

	H_2	H_2/Z_dZn (figure 2)	$(ZnH^+ + H^+)/Z_dZn$ 2nd step (figure 6)	$(ZnH^+ + H^+)/Z_dZn$ final step (figure 7)	$(ZnH^+ + H^+)/Z_dZn$
$\nu_{H–H}$	4419	4149 (−270)			
$\nu_{O–H}$			3449	3468	3822
$\nu_{Zn–H}$			1958	1956	1952

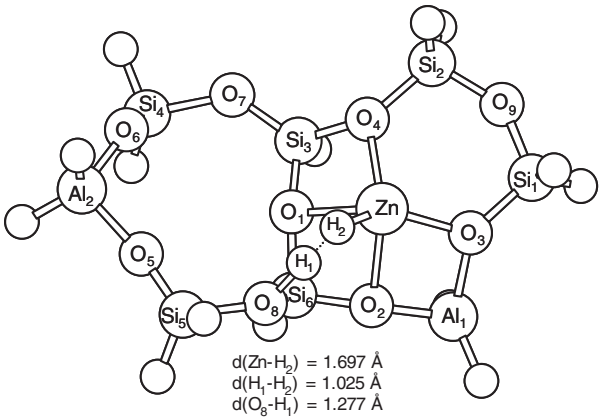

Figure 3. The transition state for H_2 dissociation on Z_dZn cluster.

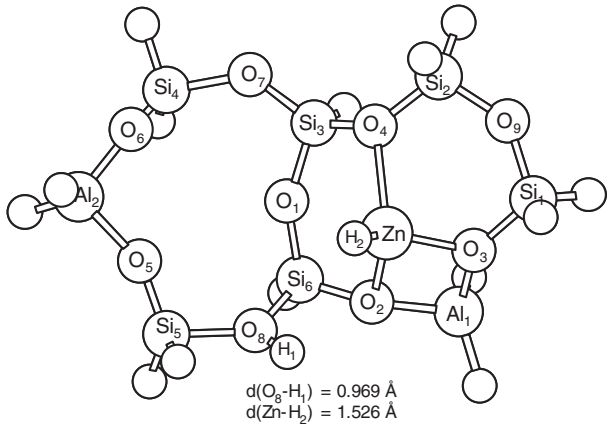

Figure 4. The first step of H_2 dissociation (local minimum for $H_{(1)}$ proton migration).

migration is shown in figure 6, while the "final" structure of the migration path is shown in figure 7. Note that in both these structures, the O–H bond is directed towards the center of the Z_dZn cluster. $Zn–H_{(2)}$ and $O–H_{(1)}$ vibrational frequencies calculated for both the structures also are very close (see table 1). At the same time, we have found in computations, additional stable structure (not shown in figures) different from the "final" structure (figure 7) only by the rotation of the $O_{(6)}–H_{(1)}$ bond around the quasilinear $Al_{(2)}–O_{(6)}–Si_{(4)}$ fragment (see figure 8 and the last column in table 1). The remarkable difference in O–H vibrational frequency ($3822\,cm^{-1}$) for this structure is due to the direction of $O_{(6)}–H_{(1)}$ bond outward the 5-ring that eliminates additional hydrogen bonding of $H_{(1)}$ with other atoms of the Z_dZn cluster. The O–H bond length, 0.965 Å, in this structure is about 0.02 Å smaller than in the structures from figures 6 and 7. The complete energy path diagram for $H_{(1)}$ migration is also shown in figure 8. The results of calculations indicate that H_2 dissociation with the subsequent migration of hydrogen atom to the second aluminum ion does not face any serious energy hindrances.

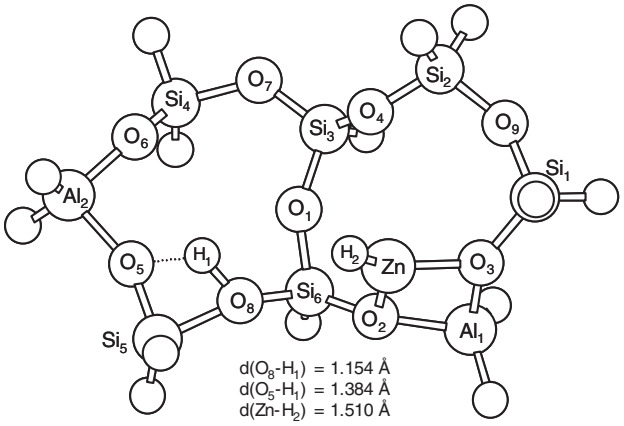

Figure 5. Transition state for $H_{(1)}$ proton transfer from $O_{(8)}$ to $O_{(5)}$.

It is appropriate at this point to compare our results with experimental data and results of other theoretical calculations especially devoted to the description of translational proton motion in zeolite H-ZSM-5. Note that the unit cell of H-ZSM-5 is large; it includes 96 tetrahedral positions (Al or Si atoms) and 192 oxygen atoms. As a consequence, up to now there are no pure periodic structure DFT studies of activation barriers for proton mobility in MFI-type zeolites. As known to us, investigations were performed in the finite cluster approximation similar to that used in this work (see

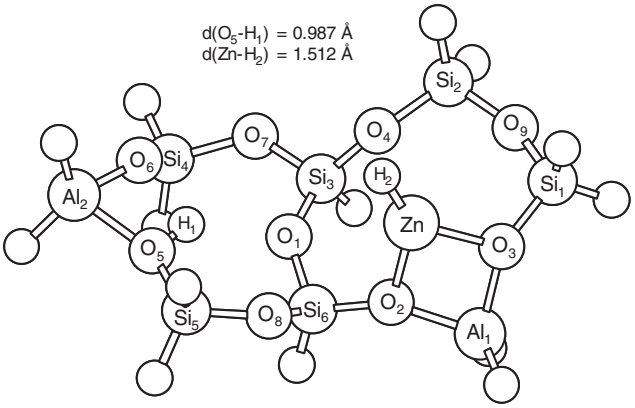

Figure 6. Second step for $H_{(1)}$ proton migration (H_2 dissociation).

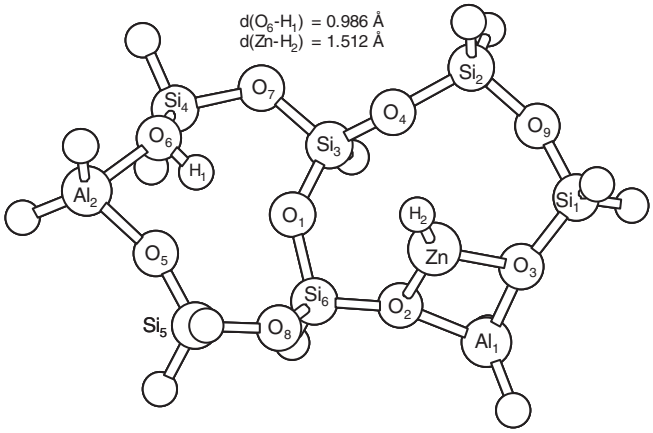

Figure 7. "Final" step for $H_{(1)}$ proton migration (H_2 dissociation).

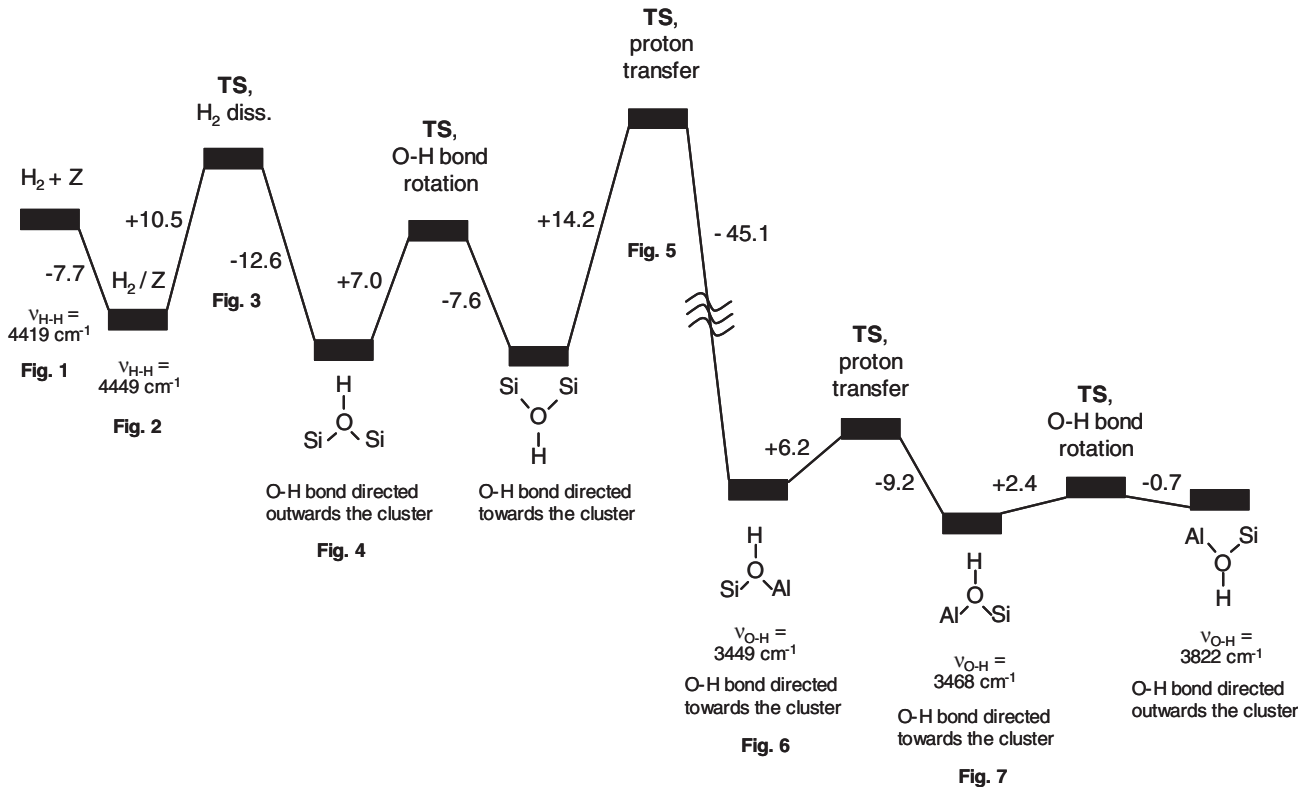

Figure 8. Energy path for $H_{(1)}$ proton migration (all values are in kcal/mol).

[22,23] and references herein) or in the combined quantum mechanics–interatomic potential function approach (QM–Pot) [24,25]. It was also shown earlier [26] that consideration of whole extended zeolite lattice is necessary for the correct explanation of deprotonation energy for different zeolites. According to reference [25], the long-range correction to the activation barriers for intersite proton motion in H-ZSM-5 zeolite with one aluminum per unit cell varies from −6.4 to +7.1 kcal/mol, while the same correction for on-site motion (proton jumps between oxygen atoms in the first coordination of an aluminum atom) was reported to be equal to +18.8 kcal/mol. These values are significant for the correct description of zeolites' acidity peculiarities and jump rates of proton translation motion, but have no effect (see figure 8) on our conclusion on the possibility of heterolytic dissociative adsorption of dihydrogen following the adsorption of dihydrogen by zinc ion. It is worth noting that for H-ZSM-5 zeolite, the experimental on-site proton jump barriers are in the range from 2.6 to 10.8 kcal/mol [27–30]. These values are at least two times smaller than those predicted from both cluster [22] and periodic [24] DFT calculations. In our calculations, we have barriers of 6.2 and 9.2 kcal/mol (figure 8) for on-site proton jumps, in agreement with experimental data. Nevertheless, we suggest that this is fortuitous, because these on-site barriers do not include the positive long-range correction mentioned above as well as a small (few kcal/mol) negative zero-point energy correction. Moreover, direct comparison of our results for ZnHZSM-5 zeolite cluster model with the results of cluster and periodic calculations for H-ZSM-5 zeolite is not quite correct, because these model systems are different.

4. Conclusion

Two adjacent five-membered rings on the wall of the straight channel of ZSM-5 zeolite sharing the common edge have been considered as a possible cationic site for Zn^{2+} with distant placing of aluminum ions. The $ZnAl_2Si_6O_9H^*_{14}$ (Z_dZn) cluster was chosen for the model DFT calculations. Molecular adsorption of dihydrogen results in the large red shift of H_2 stretching frequency equal to $-270\,cm^{-1}$. The adsorption energy was evaluated as equal to 7.7 kcal/mol. The next step is the heterolytic dissociation of adsorbed hydrogen, resulting in the migration of proton toward the oxygen ions at the distant aluminum. Simultaneously, the second hydrogen atom forms the Zn–H chemical bond. The activation energies of this step are estimated as 10.5 and 2.8 kcal/mol relative to the adsorption state or to the initial hydrogen molecule, respectively. The intermediates and transition states of subsequent steps of proton migration were also found, and it was concluded that H_2 dissociation with the subsequent migration of proton to the basic oxygen at the second aluminum atom does not face any serious energy

hindrances. Zn–H and O–H stretching frequencies were calculated for final structures, whereas the remarkable difference in O–H vibrational frequencies could be explained by hydrogen bonding in some of these structures.

Acknowledgment

The Dutch Science Foundation is gratefully acknowledged for the financial support of the collaborative Russian–Dutch Project NWO-19-0411999. G.M.Z. and A.A.S. also thank RFBR (project 00-15-97441) for the support of this study.

References

[1] A. Chatterjee and R. Vetrivel, Microporous Mater. 3 (1994) 211.
[2] D. Nachtigallova, P. Nachtigall, M. Sierka and J. Sauer, Phys. Chem. Chem. Phys. 1 (1999) 2019.
[3] M.H. Sonnemans, C. den Heijer and M. Crocer, J. Phys. Chem. 97 (1993) 440.
[4] M.J. Rice, A.K. Chakraborty and A.T. Bell, J. Catal. 186 (1999) 222.
[5] M.J. Rice, A.K. Chakraborty and A.T. Bell, J. Catal. 194 (2000) 278.
[6] A.L. Yakovlev, A.A. Shubin, G.M. Zhidomirov and R.A. van Santen, Catal. Lett. 70 (2000) 175.
[7] V.B. Kazansky, submitted to J. Catal.
[8] V.B. Kazansky and A.I. Serykh, in preparation.
[9] A.A. Shubin, G.M. Zhidomirov, A.L. Yakovlev and R.A. van Santen, J. Phys. Chem. B 105 (2001) 4928.
[10] G.M. Zhidomirov, A.A. Shubin, V.B. Kazansky, V.N. Solkan, R.A. van Santen, A.L. Yakovlev and L.A.M.M. Barbosa, in *Catalysis for Sustainable Development* (Russian–Dutch Workshop Abstracts, Novosibirsk, 22–25 June, 2002), pp. 14–17.
[11] L.A.M.M. Barbosa, G.M. Zhidomirov and R.A. van Santen, PCCP 2 (2000) 3909.
[12] L.A.M.M. Barbosa, G.M. Zhidomirov and R.A. van Santen, Catal. Lett. 77 (2001) 55.
[13] V.B. Kazansky, V.Yu. Borovkov, A.I. Serykh, R.A. van Santen and B.G. Anderson, Catal. Lett. 66 (2000) 39.
[14] V.B. Kazansky, A.I. Serykh, R.A. van Santen and B.G. Anderson, Catal. Lett. 74 (2001) 55.
[15] V.B. Kazansky, A.I. Serykh, R.A. van Santen and B.G. Anderson, submitted to Catal. Lett.
[16] V.B. Kazansky, V.Yu. Borovkov, A.I. Serykh, R.A. van Santen and P.J. Stobbelar, PCCP 1 (1999) 2881.
[17] V.B. Kazansky, A.I. Serykh and A.T. Bell, Catal. Lett. 83 (2002) 191.
[18] H. Lermer, M. Draeger, J. Steffen and K.K. Unger, Zeolites 5 (1985) 131.
[19] Revision A.11, M.J. Frisch, G.W. Trucks, H.B. Schlegel, G.E. Scuseria, M.A. Robb, J.R. Cheeseman, V.G. Zakrzewski, J.A. Montgomery Jr., R.E. Stratmann, J.C. Burant, S. Dapprich, J.M. Millam, A.D. Daniels, K.N. Kudin, M.C. Strain, O. Farkas, J. Tomasi, V. Barone, M. Cossi, R. Cammi, B. Mennucci, C. Pomelli, C. Adamo, S. Clifford, J. Ochterski, G.A. Petersson, P.Y. Ayala, Q. Cui, K. Morokuma, P. Salvador, J.J. Dannenberg, D.K. Malick, A.D. Rabuck, K. Raghavachari, J.B. Foresman, J. Cioslowski, J.V. Ortiz, A.G. Baboul, B.B. Stefanov, G. Liu, A. Liashenko, P. Piskorz, I. Komaromi, R. Gomperts, R.L. Martin, D.J. Fox, T. Keith, M.A. Al-Laham, C.Y. Peng, A. Nanayakkara, M. Challacombe, P.M.W. Gill, B. Johnson, W. Chen, M.W. Wong, J.L. Andres, C. Gonzalez, M. Head-Gordon, E.S. Replogle and J.A. Pople, *Gaussian 98* (Gaussian, Inc., Pittsburgh PA, 2001).
[20] A.D. Becke, Phys. Rev. A38 (1988) 3098; A.D. Becke, J. Chem. Phys. 98 (1993) 1372; A.D. Becke, J. Chem. Phys. 98 (1993) 5648.
[21] J. Baker, M. Muir, J. Andzelm and A. Scheiner, in *Chemical Applications of Density-Functional Theory*; B.B. Laird, R.B. Ross and T. Ziegler (eds), ACS Symposium Series 629 (American Chemical Society, Washington DC, 1996
[22] J.A. Ryder, A.K. Chakraborty and A.T. Bell, J. Phys. Chem. B 104 (2000) 6998.
[23] J.T. Fermann and S.M. Auerbach, J. Phys. Chem. A 105 (2001) 2879.
[24] M. Sierka and J. Sauer, J. Phys. Chem. B 105 (2001) 1603.
[25] M.F. Franke, M. Sierka and U. Simon, J. Sauer, PCCP 4 (2002) 5207.
[26] M. Brändle and J. Sauer, J. Am. Chem. Soc. 120 (1998) 1556.
[27] P. Sarv, T. Tuherm, E. Lippmaa, K. Keskinen and A. Root, J. Phys. Chem. 99 (1995) 13763.
[28] T. Baba, Y. Inoue, H. Shoji, T. Uematsu and Y. Ono, Microporous Mater. 3 (1995) 647.
[29] T. Baba, N. Komatsy, Y. Ono and H. Sugisawa, J. Phys. Chem. B 102 (1998) 804.
[30] H. Ernst, D. Freude, T. Mildner and H. Pfeifer, in Proc. 12th International Zeolite Conference M.M. Treacy, B.K. Marcus, M.E. Bisher and J.B. Higgins (eds) Vol. 4 (Materials Research Society, Warrendale, 1999) pp. 2955–2962.